

# Platinum-Catalyzed Hydrosilylation—Colloid Formation as the Essential Step

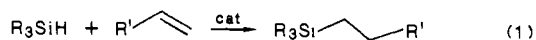
Larry N. Lewis\* and Nathan Lewis

Contribution from the General Electric Company, Corporate Research and Development Center, Schenectady, New York 12301. Received April 14, 1986

**Abstract:** In a reaction which has broad implications for many ostensibly homogeneous metal-catalyzed reduction processes, it is shown that platinum-catalyzed hydrosilylation proceeds with formation of platinum colloids. The reaction of  $\text{CODPtCl}_2$  with  $(\text{EtO})_3\text{SiH}$  demonstrates that colloid formation is the key step in hydrosilylation. Colloids are generated from the reactions of  $\text{Pt}(\text{COD})_2$  and  $\text{CODPtCl}_2$  with hydrosilanes and analyzed by light scattering, TEM, and ESCA.

Recently the problem of distinguishing between homogeneous and heterogeneous catalytic processes has come to the fore of active research.<sup>1-3</sup> A homogeneous catalyst offers the potential advantage of high selectivity while a heterogeneous system is often less selective but more active.<sup>4</sup> Work in this laboratory has examined the novel case of a proven homogeneous ruthenium catalyst which can be transformed into a ruthenium colloid.<sup>5</sup> There are many cases in which molecular compound precursors are employed as catalysts but where the exact nature of the catalytic species are unknown. Many accepted homogeneous processes are coming under renewed scrutiny with regards to the nature of the active catalytic species.

The hydrosilylation reaction, eq 1, is formally related to olefin hydrogenation. Hydrosilylation reactions are generally carried out in the presence of a transition-metal catalyst, with platinum the most active catalyst.<sup>6</sup> The accepted mechanism of plati-



num-catalyzed hydrosilylation is based on the intermediacy of platinum complexes. It is well-known that platinum and palladium phosphine complexes are catalysts for hydrosilylation.<sup>7,8</sup> Intermediates of the type  $\text{L}_2\text{M}(\text{SiR}_3)\text{H}$  can be isolated in many cases from reaction mixtures.<sup>9</sup> These observations and the fact that the phosphine complexes are quite selective, i.e., promoting asymmetric hydrosilylation of olefins,<sup>10</sup> support the homogeneous-based mechanism proposed for these systems. However, many other low valent platinum complexes are several orders of magnitude more active than the phosphine complexes. We report, for the first time, evidence that the mechanism for hydrosilylation mediated by highly active catalysts involves formation of colloidal platinum as the key step.

## Results and Discussion

The mechanism of hydrosilylation in the presence of low valent olefin-platinum complexes was investigated.  $\text{Pt}^0(\text{COD})_2$  (COD = 1,5-cyclooctadiene) was as active as the most active catalyst reported in the patent literature.<sup>11</sup> For example, the reaction of

$(\text{EtO})_3\text{SiH}$  and  $\text{Me}_3\text{Si}(\text{CH}=\text{CH}_2)$  in the presence of 10 ppm  $\text{Pt}^0(\text{COD})_2$  was exothermic after a brief induction period at 25 °C and complete within about 15 min. This corresponded to 100 000 catalyst turnovers—an unusually fast reaction for a reduction process catalyzed by a homogeneous species! In an attempt to study the nature of the active catalyst, the reaction between  $\text{Pt}^0(\text{COD})_2$  and  $(\text{EtO})_3\text{SiH}$  was examined. The colorless xylene solution of  $\text{Pt}^0(\text{COD})_2$  turned dark upon addition of the silane but remained visually clear. The solution generated by this procedure (colloid-1) was a more active catalyst than  $\text{Pt}(\text{COD})_2$  itself. For example, in the hydrosilylation reaction between  $\text{Et}_3\text{SiH}$  and  $\text{Me}_3\text{Si}(\text{CH}=\text{CH}_2)$  at 70 °C, in 7.5 min 26% conversion to product occurred in the presence of  $\text{Pt}(\text{COD})_2$  whereas 85.5% conversion occurred in the presence of colloid-1.

Transmission electron microscopy (TEM) was used to analyze colloid-1. In Figure 1, light colored ellipsoids can be seen which were shown by X-ray spectroscopy to be rich in platinum whereas the background was devoid of platinum but was rich in silicon. The light color regions suggest a high surface area, honeycomb structure. The appearance of these particles stands in sharp contrast to the lower surface area, hard spheres shown in Figure 2 for  $\text{H}_2\text{PtCl}_6$  in isopropanol (Speier's catalyst). Chloroplatinic acid was the first "homogeneous" catalyst reported for hydrosilylation<sup>12</sup> but is an order of magnitude less active than  $\text{Pt}(\text{COD})_2$ . The spheres in Figure 2 have a mean diameter of 830 Å.<sup>13,14</sup> Dynamic light scattering of Speier's catalyst in solution shows non-Gaussian distribution of particles with a mean size of 530 Å.<sup>15</sup> Thus, these active catalysts contain colloidal platinum with the more active catalyst having the higher surface area.

Further details of the mechanism of hydrosilylation in the presence of an active catalyst were obtained by studying the reaction of  $\text{CODPt}^{\text{II}}\text{Cl}_2$  with  $(\text{EtO})_3\text{SiH}$ , eq 2. When 6 equiv  $\text{CODPtCl}_2 + x\text{s}(\text{EtO})_3\text{SiH} \xrightarrow{\text{CH}_2\text{Cl}_2} [\text{Pt}^0]_x + \text{H}_2\uparrow + \text{ClSi}(\text{OEt})_3 + \text{c-C}_8\text{H}_{14} + \text{c-C}_8\text{H}_{16}$  (2) colloid-2

of triethoxysilane were added to a  $\text{CH}_2\text{Cl}_2$  solution of  $\text{CODPt}^{\text{II}}\text{Cl}_2$ , reaction occurred in which  $\text{H}_2$  gas was evolved, and colloid-2 was

(1) Hamlin, J. E.; Hirai, K.; Millan, A.; Maitlis, P. M. *J. Mol. Catal.* **1980**, *7*, 543.

(2) Crabtree, R. H.; Mellea, M. F.; Mihelcic, J. M.; Quirk, J. M. *J. Am. Chem. Soc.* **1982**, *104*, 107. Anton, D. R.; Crabtree, R. H. *Organometallics* **1983**, *2*, 855.

(3) Crabtree, R. H.; Demon, P. C.; Eden, D.; Mihelcic, J. M.; Parnell, C. A.; Quirk, J. M. Morris, G. E. *J. Am. Chem. Soc.* **1982**, *104*, 6994.

(4) Parshall, G. W. *Homogeneous Catalysis*; Wiley: New York, 1980.

(5) Lewis, L. N. *J. Am. Chem. Soc.* **1986**, *108*, 743.

(6) Harrod, J. F.; Chalk, A. J. In *Organic Syntheses Via Metal Carbonyls*; Wender, I.; Pino, P., Eds.; Wiley: New York, 1977; Vol. 2, p 673.

(7) Eaborn, C.; Boff, R. W. In *The Bond to Carbon*; MacDiarmid, A. G., Ed.; Marcel Dekker: 1968; Vol. 1.

(8) Lukevics, E.; Belyakova, Z. V.; Pomerantseva, M. G.; Voronkov, M. G. In *J. Organomet. Chem. Library*; Seyferth, D., Ed.; Elsevier: 1977, Vol. 5.

(9) Yamamoto, K.; Hayashi, T.; Kumada, M. *J. Organomet. Chem.* **1971**, *28*, C37.

(10) Yamamoto, K.; Hayashi, T.; Zembayashi, M.; Kumada, M. *J. Organomet. Chem.* **1976**, *118*, 161.

(11) (a) Willing, D. N. U.S. Patent 3 419 593, 1968. (b) Karstedt, B. D. U.S. Patent 3 775 452, 1973. (c) Ashby, B. A.; Modic, F. J. U.S. Patent 4 288 345, 1981.

(12) Speier, J. L. *Adv. Organomet. Chem.* **1979**, *17*, 407.

(13) Electron diffraction analysis of the particles from chloroplatinic acid in isopropanol, Figure 2, showed a diffraction pattern which indexed to polycrystalline platinum. See ASTM X-Ray Powder Diffraction File, card no. 4-0802. On the other hand, the particles of colloid-1, Figure 1, did not show a well-defined diffraction pattern consistent with an amorphous material for colloid-1.

(14) Particle distribution analyses were performed by employing the Zeiss IBAS image analysis system.

(15) The Nicomp Model 270 submicron particle analyzer used in this study provides two means of analyzing solutions for particle distribution. One method employs the conventional conversion of the autocorrelation function into a Gaussian function. The second method is a Pacific Scientific Corp. proprietary program which makes no assumption about the nature of the function, e.g., Gaussian, bimodal, etc. Both methods of analysis were used in all cases with good agreement.

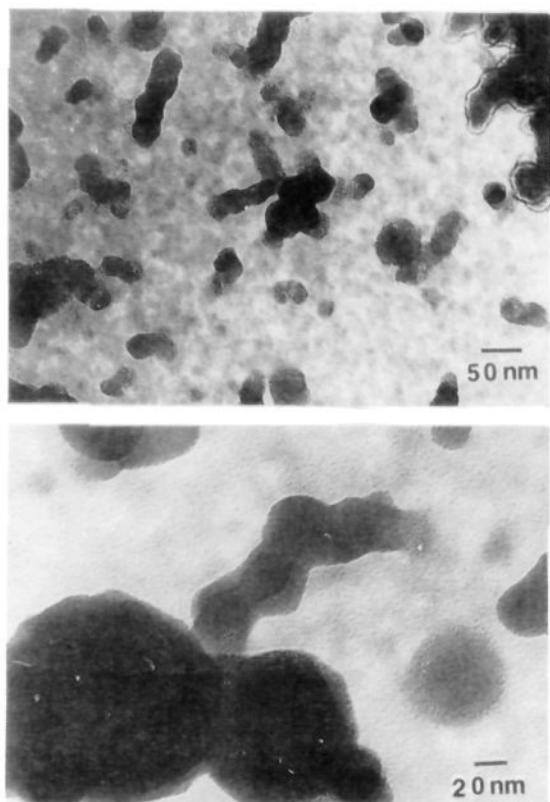


**Figure 1.** Transmission electron micrograph of colloid-1:  $\text{Pt}(\text{COD})_2 + 50(\text{EtO})_3\text{SiH} (+ \text{C}_6\text{D}_6) \rightarrow \dots$ . Note light colored ellipsoids. These areas are rich in platinum as determined by X-ray spectroscopy. The background is mostly silicon.

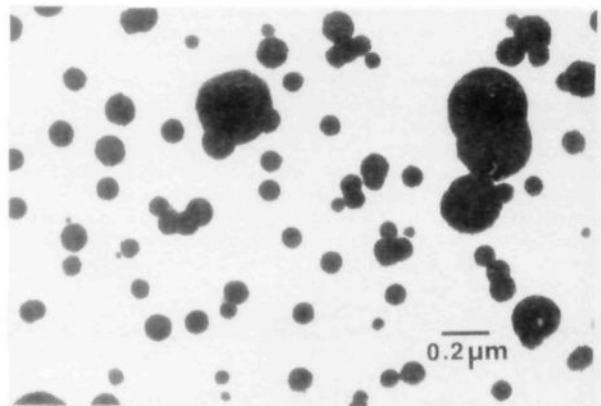


**Figure 2.** Transmission electron micrograph of  $\text{H}_2\text{PtCl}_6$  in isopropyl alcohol (Speier's catalyst).

formed. As shown in Figure 3, for the test reaction of  $\text{Me}_3\text{Si}(\text{CH}=\text{CH}_2)$  with  $(\text{EtO})_3\text{SiH}$ , colloid-2 was more active than  $\text{CODPtCl}_2$  itself, a result reminiscent of the relative activities of  $\text{Pt}(\text{COD})_2$  and colloid-1. Particularly noteworthy was the activity of colloid-2 in the early phases of the test reaction. Whereas in 12 min in the presence of  $\text{CODPtCl}_2$  18% conversion occurred, there was 35% conversion in the presence of colloid-2.

The reaction of eq 2 was studied in greater depth. Upon addition of  $(\text{EtO})_3\text{SiH}$  to a  $\text{CH}_2\text{Cl}_2$  solution of  $\text{CODPtCl}_2$ , no reaction was immediately evident.  $^1\text{H}$  and  $^{13}\text{C}$  NMR analysis immediately after addition of silane confirmed that no reaction had occurred in the colorless solution. Furthermore, light scattering showed that no particles ( $>15 \text{ \AA}$ ) were present in the solution. After 1 h, a yellow color developed, and gas evolution was noted. GCMS analysis showed that the evolved gas was  $\text{H}_2$ . At this point, light scattering showed a narrow distribution of particles with a mean diameter of  $40 \text{ \AA}$ .  $^1\text{H}$  and  $^{13}\text{C}$  NMR

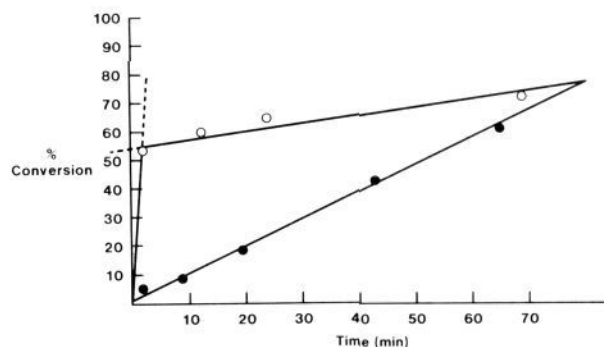


**Figure 3.** Relative rates for platinum-catalyzed hydrosilylation for the reaction  $(\text{EtO})_3\text{SiH} + \text{Me}_3\text{Si}(\text{CH}=\text{CH}_2)$  ( $25^\circ\text{C}$ , 100 ppm catalyst)  $\rightarrow (\text{EtO})_3\text{SiCH}_2\text{CH}_2\text{SiMe}_3$ . Note initial fast reaction in the presence of colloid-2 (O) vs.  $\text{CODPtCl}_2$  (●). The reaction catalyzed by colloid-2 reached 100% conversion at 309 min, while the reaction catalyzed by  $\text{CODPtCl}_2$  reached 97% conversion in 19 h.

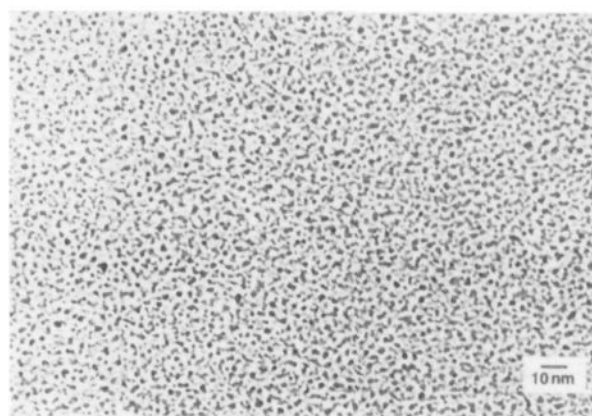


**Figure 4.** Transmission electron micrograph of colloid-2:  $\text{CODPtCl}_2 + 6(\text{EtO})_3\text{SiH} (+ \text{CH}_2\text{Cl}_2) \rightarrow \dots$

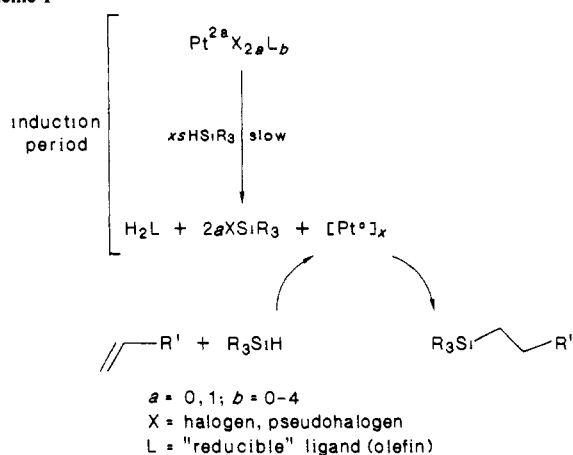
analyses showed that the silane and  $\text{CODPtCl}_2$  were consumed in the reaction and that no new platinum-olefin complex formed; there were no new resonances with  $^{195}\text{Pt}$  satellites. Furthermore, the  $^{195}\text{Pt}$  NMR showed that the  $\text{CODPtCl}_2$  resonance was gone but that no new peak was formed. The  $^1\text{H}$  and  $^{13}\text{C}$  NMR showed new ethyl resonances and peaks assigned to cyclooctene and cyclooctane (vs. authentic samples).  $^{29}\text{Si}$  NMR and GCMS confirmed the formation of  $\text{ClSi}(\text{OEt})_3$ . The reaction of eq 2 was followed by IR which revealed that  $\text{Pt}-\text{Cl}$  ( $\nu_{\text{Pt}-\text{Cl}}$   $350 \text{ cm}^{-1}$ ) and  $\text{SiH}$  were consumed in the course of the reaction and that  $\text{SiCl}$  was formed ( $590$  and  $530 \text{ cm}^{-1}$ ). The sequence of events described was observed when  $\text{MeCl}_2\text{SiH}$  was used in place of  $(\text{EtO})_3\text{SiH}$  in eq 2. New methyl resonances were observed by NMR, and cyclooctene and cyclooctane were observed as well.

The structures of the colloids were investigated. Colloid-2 was examined by TEM (Figure 4) which showed platinum particles with a mean size of  $23 \text{ \AA}$  (range from  $6 \text{ \AA}$  to  $60 \text{ \AA}$ ).<sup>14</sup> These results confirm that a platinum colloid was formed by hydrosilane reduction of  $\text{CODPtCl}_2$  in  $\text{CH}_2\text{Cl}_2$ . Formation of a stable colloid of platinum in nonaqueous-nonanol media is unknown and unheard of in the platinum literature.<sup>16</sup> ESCA analysis confirmed that colloid-2 had characteristics distinct from bulk metal. The  $\text{Pt } 4f_{7/2}$  binding energy for colloid-2 was  $72.24 \text{ eV}$ . Bulk platinum metal has a binding energy of  $71.0 \text{ eV}$  while this work showed that  $\text{CODPtCl}_2$  was  $72.45 \text{ eV}$  (cf.  $\text{PtCl}_2$   $73.3 \text{ eV}$ ).<sup>17</sup> The binding energy in colloid-2 was higher than bulk metal, an observation consistent with the idea that there are fewer delocalized "band"

(16) Koelmans, H.; Overbeek, J. Th. G. *Disc. Farad. Soc.* **1954**, *18*, 52. Gaines, G. L.; General Electric, C.R.D., personal communication.

(17) Wagner, C. D.; Riggs, W. M.; Davis, L. E.; Moulder, J. F.; Muilenberg, G. E. *Handbook of X-ray Photoelectron Spectroscopy*; Perkin Elmer: Eden Prairie, MN, 1979.

Scheme I



electrons in the colloid compared to bulk metal.

The colloids' structures were further probed by the reaction with CO. A chloroplatinic acid-isopropanol solution was reacted with carbon monoxide. Infrared analysis showed a CO band at 2090  $\text{cm}^{-1}$  consistent with a terminal carbonyl. The reaction of colloid-2 with CO was also examined. There was no reaction between  $\text{CODPtCl}_2$  and CO. However, subsequent to a carbon monoxide purge through a solution of colloid-2, the IR revealed  $\nu_{\text{CO}}$  bands at 2050 (s) and 1880 (m). The latter band agrees with the reported IR for a bridging carbonyl on a platinum surface.<sup>18</sup> The results of the reaction of CO with colloid-2 are consistent with the presence of adjacent platinum binding sites and may suggest a high surface area. The chloroplatinic acid result suggests that CO bound to the "hard sphere" type colloid can bind to terminal sites, consistent with a low surface area structure.

Recently Crabtree<sup>2</sup> and Whitesides<sup>19</sup> have shown that mercury can be used as a selective poison for heterogeneous (colloidal) catalysts while homogeneous (molecular compounds) are unaffected by Hg. The effect of mercury on the activity of three catalysts from the present study was measured;  $\text{CODPtCl}_2$ , colloid-2, and Speier's catalyst. Solutions of olefin ( $\text{Me}_3\text{Si}(\text{CH}=\text{CH}_2)$ ) and catalyst were stirred with and without mercury present. The addition of silane ( $(\text{EtO})_3\text{SiH}$ ) initiated the reaction. In all three cases, prereaction with mercury led to complete poisoning of the catalysts, while in the absence of Hg the reactions proceeded (see Experimental Section). These results confirm that the active component of the hydrosilylation reaction in the presence of these catalysts is heterogeneous.

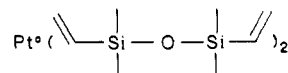
The proposed mechanism for hydrosilylation (see Scheme I) is based on the formation of colloidal platinum as the active catalyst. It is well-known that an induction period precedes the exothermic hydrosilylation reaction, and it has been proposed that during the induction period, the active catalyst forms.<sup>6,12</sup> It is particularly noteworthy that the induction period is sharply reduced (Figure 3) when the colloidal catalysts are employed. In addition, the colloids are more active than the compounds from which they are derived. In Scheme I, if  $\text{CODPtCl}_2$  is used as an example ( $L_b = 1,5$  cyclooctadiene,  $a = 1$ ,  $\text{X} = \text{Cl}$ ), the slow step is the first addition of hydrosilane to the metal because no platinum-olefin intermediates are observed. The subsequent reduction steps, including formation of the colloid, are fast. Once colloid platinum is formed, further production of  $\text{H}_2$  from the silane proceeds at a fast rate so that cyclooctene is eventually converted to cyclooctane.

### Conclusions and Predictions

This work has shown that an accepted homogeneous catalytic process is actually brought about by colloids. It is more than likely

that the Chalk/Harrod mechanism is operative for authentic homogeneous hydrosilylation catalysts such as  $(\text{Ph}_3\text{P})_4\text{Pt}$ . However, we propose that the colloid based mechanism is the most important one, where formation of  $\text{Pt}^0$ , free of ligands, is readily achieved. Reduction processes catalyzed by homogeneous metal complexes should be reexamined in light of the present results. In particular, where reduction of ligand and metal are feasible processes, colloid catalyst intermediates should be considered.

Work in these laboratories and a recent report by the Dow Corning group<sup>20</sup> have shown that a very active platinum hydrosilylation catalyst from the patent literature<sup>11b</sup> is indeed a platinum zero complex



The mechanism of hydrosilylation catalyzed by this complex is analogous to that catalyzed by  $\text{Pt}(\text{COD})_2$ —reduction of the ligand by hydrosilane with concomitant formation of a platinum colloid. Furthermore, colloid formation can account for the high activity of a recently reported photo hydrosilylation catalyst,  $\text{CODPtPh}_2$ .<sup>21</sup> Work in the literature<sup>22</sup> has shown that  $L_2\text{PtR}_2$  complexes undergo reductive elimination to yield  $L_2\text{Pt}^0 + \text{R-R}$ . Our work has shown that irradiation of solutions of  $\text{CODPtPh}_2$  produces free COD, biphenyl, and a dark color suggestive of platinum colloid formation.

### Experimental Section

**General Methods.** Most operations were carried out in air under ambient conditions. Where inert atmosphere was required, a nitrogen filled Vacuum Atmosphere glovebox was employed. NMR spectra were recorded by using either a Varian FT 80A NMR spectrometer ( $^{13}\text{C}$ , 20 MHz;  $^{29}\text{Si}$ , 15.801 MHz), a Varian EM 390 NMR spectrometer ( $^1\text{H}$ , 90 MHz), or a Varian XL 300 NMR spectrometer ( $^{13}\text{C}$ , 75.43 MHz;  $^{29}\text{Si}$ , 59.3 MHz,  $^{195}\text{Pt}$ , 64.12 MHz). Infrared measurements were made by using a Perkin Elmer Model 598 IR spectrometer. Gas chromatography was performed by using an HP 5830A gas chromatograph employing 6' 3% OV 101 columns. GCMS analysis was performed by using a Varian MAT 311A instrument. Dynamic light scattering (DLS) measurements were made by using a Nicomp Model 270 submicron particle analyzer at 23 °C.<sup>15</sup> Transmission electron micrographs (TEM) were carried out by using a Hitachi H-600 analytical electron microscope operated at 100 KeV. Samples were prepared by evaporating solutions onto a copper support grid. ESCA measurements were made by using a Surface Science Laboratories SSSX-100 small spot ESCA. The carbon 1s binding energy of 284.6 eV was used as an internal standard.

**Materials.** Silicon compounds were obtained from either Silar or Petrarch;  $(\text{EtO})_3\text{SiH}$  and  $\text{MeCl}_2\text{SiH}$  were purified by distillation.  $\text{CODPtCl}_2$ <sup>23</sup> and  $\text{Pt}(\text{COD})_2$ <sup>24</sup> were prepared via literature procedures.

**Activity of  $\text{Pt}(\text{COD})_2$ .** A stock solution of equimolar amounts of  $(\text{EtO})_3\text{SiH}$  and  $\text{Me}_3\text{Si}(\text{CH}=\text{CH}_2)$  was prepared by combining  $(\text{EtO})_3\text{SiH}$  (2 mL, 10.7 mmol),  $\text{Me}_3\text{Si}(\text{CH}=\text{CH}_2)$  (1.55 mL, 10.7 mmol), and decane (internal standard, 0.5 mL). To the above stock solution (0.5 mL) was added  $\text{Pt}(\text{COD})_2$  (0.5  $\mu\text{L}$  of a solution—0.019 g, 0.046 mmol in 1 mL toluene—10 ppm).

**Preparation and Activity of Colloid-1.** A xylene solution (1 mL) of  $\text{Pt}(\text{COD})_2$  (0.015 g, 0.036 mmol) was combined with  $(\text{EtO})_3\text{SiH}$  (0.38 mL, 2.02 mmol). The initially colorless solution turned black (colloid-1) upon addition of silane. The relative activities of  $\text{Pt}(\text{COD})_2$  and colloid-1 were compared. A stock solution was prepared which contained  $\text{Et}_3\text{SiH}$  (2.2 mL, 13.8 mmol),  $\text{Me}_3\text{Si}(\text{CH}=\text{CH}_2)$  (2 mL, 13.8 mmol), and decane (internal standard, 0.5 mL). To the stock solution (0.5 mL) was added  $\text{Pt}(\text{COD})_2$  (5  $\mu\text{L}$  of a solution—0.019 g, 0.046 mmol in 1 mL of toluene—100 ppm Pt). To a second aliquot of the stock solution (0.5 mL) was added colloid-2 solution (8.3  $\mu\text{L}$  of solution prepared above, 100 ppm Pt). The stock solutions containing  $\text{Et}_3\text{SiH}$ ,  $\text{Me}_3\text{Si}(\text{CH}=\text{CH}_2)$ , and catalyst were heated to 70 °C in closed containers, and the percent conversion was measured by GC.

(20) Lo, P. Y.; Chandra, G. *Am. Chem. Soc. Nat. Mtg. INOR Abstracts* 36, New York, Spring 1986.

(21) Drahnak, T. J. U.S. Patent 4 530 879, 1985.

(22) (a) Paonessa, R. S.; Prignano, A. L.; Troglor, W. C. *Organometallics* **1985**, *4*, 647. (b) McDermott, J. X.; White, J. F.; Whitesides, G. M. *J. Am. Chem. Soc.* **1976**, *98*, 6521.

(23) Drew, D.; Doyle, J. R. *Inorg. Synth.* **1972**, *13*, 47.

(24) Spencer, J. L. *Inorg. Synth.* **1979**, *19*, 213. Herberich, G. E.; Hessner, B. *Z. Naturforsch., B: Anorg. Chem., Org. Chem.* **1979**, *34B*, 638.

(18) Beden, B.; Bewick, A.; Kunitatsu, K.; Lamy, C. *J. Electroanal. Chem.* **1982**, *142*, 345.

(19) Whitesides, G. M.; Hackett, M.; Brainard, R. L.; Lavalleye, J. P. M.; Sowinski, A. F.; Izumi, A. N.; Moore, S. S.; Brown, D. W.; Staudt, E. M. *Organometallics* **1985**, *4*, 1819.

Table I

catalyst	Hg present	% conversion	
		5 min	1 h
CODPtCl <sub>2</sub> (CH <sub>2</sub> Cl <sub>2</sub> )	-	0.6	7.2
CODPtCl <sub>2</sub> (CH <sub>2</sub> Cl <sub>2</sub> )	+	0	0
colloid-2 (CH <sub>2</sub> Cl <sub>2</sub> )	-	43.7	68.7
colloid-2 (CH <sub>2</sub> Cl <sub>2</sub> )	+	0	0.2
H <sub>2</sub> PtCl <sub>6</sub> (isopropyl alcohol)	-	10.9	34.3
H <sub>2</sub> PtCl <sub>6</sub> (isopropyl alcohol)	+	0	0

**Preparation of Colloid-2.** Colloid-2 was prepared by dissolving CODPtCl<sub>2</sub> (0.065 g, 0.17 mmol) in 2 mL of CH<sub>2</sub>Cl<sub>2</sub> and then adding (EtO)<sub>3</sub>SiH (0.2 mL, 1.06 mmol). Over the course of 2 h, the initially colorless solution changed color from yellow and then to orange. Gas

evolution began after 1 h. A variant of colloid-2 was prepared by combining CODPtCl<sub>2</sub> (0.0304 g, 0.0812 mmol) in 1 mL of CH<sub>2</sub>Cl<sub>2</sub> with MeCl<sub>2</sub>SiH (0.05 mL, 0.48 mmol).

**Effect of Mercury.** Me<sub>3</sub>Si(CH=CH<sub>2</sub>) (0.5 mL, 3.45 mmol) and 100 ppm (final concentration) of a platinum solution (see below) were combined in a vial with a stir bar. The solutions were stirred for 7<sup>1</sup>/<sub>2</sub> h in air with or without Hg (large excess). (EtO)<sub>3</sub>SiH (0.65 mL, 3.45 mmol) was added, and then conversions were monitored by GC (Table I).

**Acknowledgment.** Dr. Mike Burrell is acknowledged for carrying out the ESCA measurements. Jim Grande performed the particle distribution analyses. Dr. Elizabeth Williams and Paul Donahue performed some of the NMR measurements. Hans Grade made the GCMS measurements. Professors Mark Wrighton, M.I.T., Robert Crabtree, Yale, and Dr. Robert Faltnyk, N.B.S., are acknowledged for helpful discussions.

## Solid-State Oxygen-17 Nuclear Magnetic Resonance Spectroscopic Studies of Zeolites and Related Systems. 1<sup>§</sup>

Hye Kyung C. Timken,<sup>†</sup> Gary L. Turner,<sup>†</sup> Jean-Pierre Gilson,<sup>†\*</sup> L. B. Welsh,<sup>†</sup> and Eric Oldfield<sup>\*†</sup>

Contribution from the School of Chemical Sciences, University of Illinois at Urbana—Champaign, Urbana, Illinois 61801, and Signal Research Center, Inc., Des Plaines, Illinois 60017. Received January 15, 1986

**Abstract:** We have obtained static, "magic-angle", and "variable-angle" sample-spinning <sup>17</sup>O NMR spectra of <sup>17</sup>O-labeled A, Y, and dealuminated Y zeolites at 67.8 and 48.8 MHz (corresponding to magnetic field strengths of 11.7 and 8.45 T). Our results indicate that the ranges of <sup>17</sup>O nuclear quadrupole coupling constants ( $e^2qQ/h$ ) of the Si[<sup>17</sup>O]Al and Si[<sup>17</sup>O]Si fragments are 3.1–3.2 and 4.6–5.2 MHz, respectively, in general agreement with those predicted on the basis of the empirical correlation presented previously (Schramm, S.; Oldfield, E. *J. Am. Chem. Soc.* **1984**, *106*, 2502). The asymmetry parameters are 0.2 for Si[<sup>17</sup>O]Al and 0.1 for Si[<sup>17</sup>O]Si. The isotropic chemical shifts of the Si[<sup>17</sup>O]Al fragments are in the range of 31–45 ppm relative to H<sub>2</sub>O, while those of the Si[<sup>17</sup>O]Si fragments are in the range of 44–57 ppm.

There has recently been considerable interest in the use of <sup>27</sup>Al and <sup>29</sup>Si "magic-angle" sample-spinning (MASS) nuclear magnetic resonance (NMR) spectroscopy to study the structures of zeolites and other framework aluminosilicates.<sup>1–6</sup> The <sup>29</sup>Si NMR spectra of these systems can exhibit up to five resonances, depending on the number of next-nearest-neighbor aluminums. As a result, <sup>29</sup>Si MASS NMR techniques can be used to determine the composition of the aluminosilicate framework,<sup>2,3</sup> in addition to providing information on silicon–aluminum ordering.<sup>3,4</sup> <sup>27</sup>Al MASS NMR has been shown to be a sensitive technique for determining the coordination of aluminum,<sup>7</sup> and probing the location of Al atoms in chemically treated zeolites,<sup>5</sup> and for the quantitative determination of Al.<sup>6</sup>

Oxygen, the last major framework nucleus of zeolites, has received only a cursory examination so far,<sup>8</sup> because its NMR active isotope has a low natural abundance. Since it is the most abundant element in the earth's crust and is the main constituent of zeolites, the possibilities of carrying out detailed <sup>17</sup>O NMR studies of zeolites are particularly attractive. In this paper, we report the first comprehensive investigation of <sup>17</sup>O NMR of A and Y zeolites by means of static, MASS, and VASS ("variable-angle" sample spinning<sup>9</sup>) NMR techniques. We believe that determination of the <sup>17</sup>O isotropic chemical shifts ( $\delta$ ), nuclear

quadrupole coupling constants ( $e^2qQ/h$ ) and electric field gradient tensor asymmetry parameters ( $\eta$ ) should provide valuable supplementary information on zeolite structure, as we have seen recently for the <sup>17</sup>O NMR of pure SiO<sub>2</sub> (low cristobalite: Janes, N.; Oldfield, E. *J. Am. Chem. Soc.* **1986**, *108*, 5743). In this paper we present our findings for the two chemically distinct oxygen species (Si[<sup>17</sup>O]Si and Si[<sup>17</sup>O]Al) of Na-, NH<sub>4</sub>-, and Ba-exchanged Y zeolites, and for Na–A and dealuminated Na–Y. Our results indicate that the electronic structure around oxygen in the Si–O–Si fragments is close to that in low cristobalite, while that in the Si–O–Al fragment is considerably more ionic, as predicted on the basis of the empirical electronegativity and quadrupole

(1) Lippmaa, E.; Mägi, M.; Samoson, A.; Tarmak, M.; Engelhardt, G. *J. Am. Chem. Soc.* **1981**, *103*, 4992.

(2) Engelhardt, G.; Lohse, U.; Lippmaa, E.; Tarmak, M.; Mägi, M. *Z. Anorg. Allg. Chem.* **1981**, *482*, 49.

(3) Klinowski, J.; Ramdas, S.; Thomas, J. M.; Fyfe, C. A.; Hartman, J. S. *J. Chem. Soc., Faraday Trans. 2* **1982**, *78*, 1025.

(4) Melchior, M. T.; Vaughan, D. E. W.; Jacobson, A. J. *J. Am. Chem. Soc.* **1982**, *104*, 4859.

(5) Fyfe, C. A.; Gobbi, G. C.; Hartman, J. S.; Klinowski, J.; Thomas, J. M. *J. Phys. Chem.* **1982**, *86*, 1247.

(6) Fyfe, C. A.; Gobbi, G. C.; Klinowski, J.; Thomas, J. M.; Ramdas, S. *Nature (London)*, **1982**, *296*, 530.

(7) Mueller, D.; Hoebbel, D.; Gessner, W. *Chem. Phys. Lett.* **1981**, *84*, 25.

(8) (a) Klinowski, J.; Thomas, J. M.; Ramdas, S.; Fyfe, C. A.; Gobbi, G. C. "Second Workshop on the Adsorption of Hydrocarbons in Microporous Sorbents", Eberswalde, G. D. R., 1982; Vol. 2, Suppl. (b) Klinowski, J. *Prog. NMR Spectrosc.* **1984**, *16*, 237.

(9) Ganapathy, S.; Schramm, S.; Oldfield, E. *J. Chem. Phys.* **1982**, *77*, 4360.

<sup>§</sup>This work was supported in part by DOE Grant No. DE-FG22-83PC60779, and in part by the U.S. National Science Foundation Solid-State Chemistry Program (Grant DMR 83-11339).

<sup>†</sup>University of Illinois at Urbana—Champaign.

<sup>‡</sup>Signal Research Center.

<sup>\*</sup>Present address: W. R. Grace & Co., Davison Chemical Division, Washington Research Center, Columbia, MD 21044.